ISSN: 0067-2904

Physical and Electrochemical Characterization of Functionalized Multiwall Carbon Nanotubes Embedded with Polypyrrole/Gold Nanoparticles

Dhulfiqar S. Mutashar[1,2*], Wasan R. Saleh[1], Ilham A. khalaf [3]
[1] *Department of Physics, College of Science, University of Baghdad, Baghdad, Iraq*
[2]*Department of Applied Science, University of Technology, Baghdad, Iraq*
[3]*Corporation of Research and Industrial Development, Iraq*

Received: 6/5/2023 Accepted: 25/10/2023 Published: 30/12/2024

Abstract

In this study, the indium tin oxide (ITO) electrode was modified, physical and electrochemical characterization were studied to be used in some biosensor applications. Using the drop-casting method, functionalized Multiwall Carbon Nanotubes, Polypyrrole, and gold nanoparticles (f-MWCNTs-AuNP-PPy) were efficiently coated on the surface of an ITO electrode. Fourier transform of infrared radiation (FTIR) and field emission scanning electron microscopy (FE-SEM) were utilized to describe the microscopic structure and morphogenesis of the generated films at the ITO electrode's surface. Cyclic voltammetry (CV) and electrochemical impedance spectroscopy (EIS) were used to assess the electroanalytical performance of electrodes after modification. The f-MWCNTs-AuNPs-PPy distribution on the ITO electrode was improved by studying the effect of adding gold nanoparticles and varying polymer concentrations on the film distribution. Electrodes were tested with bare ITO electrodes as well as electrodes modified with f-MWCNTs, f-MWCNTs-PPy, and f-MWCNTs-AuNPs-PPy. The results revealed that nanoparticles distributed on the surface of the modified electrode reduced its impedance by roughly 40% for f-MWCNTs, 75% for f-MWCNTs-PPy, and 95% for f-MWCNTs-PPy-AuNPs. The equivalent circuit was appropriately matched in three situations (f-MWCNTs, f-MWCNTs-PPy, and f-MWCNTs-PPy-AuNPs). The transmission line model, which shows the impedance sensitivity of a diffusion process was utilized to describe the film properties. Nanoparticles enhance electrochemical performance by increasing electrochemical active surface area and allowing electron transport from the redox probe (Ferrocene/ Ferrocenium) to the ITO electrode.

Keywords: Multiwall Carbon Nanotubes, Polypyrrole, gold nanoparticles, electrochemical impedance spectroscopy, cyclic voltammetry

التوصيف الفيزيائي والكهروكيميائي لأنابيب الكاربون النانوية متعددة الجدران المفعلة والمدمجة مع بولي بيرول/ جسيمات الذهب النانوي

ذوالفقار شجاع مطشر[2,1*], وسن رشيد صالح [1], ألهام عبد الهادي خلف [3]
[1]قسم الفيزياء, كلية العلوم, جامعة بغداد
[2]قسم العلوم التطبيقية, الجامعة التكنولوجية
[3]مركز الرازي, هيأة البحث والتطوير الصناعي, وزارة الصناعة والمعادن

*Email: mutshar1990@gmail.com

الخلاصة

في هذه الدراسة، تم تعديل قطب ITO للتوصيف الفيزيائي والكهروكيميائي لبعض تطبيقات أجهزة الاستشعار البيولوجي. باستخدام طريقة الصب المسقط، تم طلاء أنابيب الكربون النانوية متعددة الجدران المفعلة، والبولي بيرول، وجسيمات الذهب النانوية (f–MWCNTs–AuNP–PPy) بكفاءة على سطح قطب ITO. تم استخدام تحويل فورير للأشعة تحت الحمراء (FTIR) والمجهر الألكتروني لمسح الانبعاث الميداني (FE–SEM) لوصف التركيب المجهري وتشكيل الأفلام المتولدة على سطح القطب الكهربائي ITO. تم استخدام قياس الجهد الدوري (CV) والتحليل الطيفي للمقاومة الكهروكيميائية (EIS) لتقييم الأداء التحليلي الكهربائي للأقطاب الكهربائية بعد التعديل. تم تحسين توزيع مركب f–MWCNTs–AuNPs–PPy على قطب ITO من خلال دراسة تأثير إضافة جسيمات الذهب النانوية وتراكيز البوليمر المختلفة على توزيع الفيلم. تم اختبار هذه الأقطاب الكهربائية باستخدام أقطاب ITO المجردة بالإضافة إلى ألاقطاب الكهربائية المعدلة باستخدام f–MWCNTs وf–MWCNTs–PPy وf–MWCNTs–AuNPs–PPy. كشفت النتائج أن الجسيمات النانوية الموزعة على سطح القطب المعدل قلت ممانعتها بحوالي 40% بالنسبة لـ f–MWCNTs، و75% بالنسبة لـ f–MWCNTs–PPy، و95% بالنسبة لـ f–MWCNTs–PPy–AuNPs. تمت مطابقة الدائرة المكافئة بشكل مناسب في ثلاث حالات (f–MWCNTs و f–MWCNTs–PPy و f–MWCNTs–PPy–AuNPs). لوصف خصائص الفيلم، تم استخدام نموذج خط النقل، الذي يوضح حساسية الممانعة لعملية الانتشار. تعمل الجسيمات النانوية على تحسين الأداء الكهروكيميائي عن طريق زيادة مساحة السطح الكهروكيميائي النشط والسماح بنقل الإلكترونات من مسبار الأكسدة والاختزال (الفيروسين/الفيروسينيوم) إلى قطب ITO.

1. Introduction

Carbonaceous compound-based electrode materials are frequently employed as working electrodes in electrochemistry and electroanalysis because of their special characteristics, such as different surface chemistry, reduced resistivity, and chemical inertness, which make them an excellent choice for determining different substances in the electrocatalytic area [1-5]. Furthermore, in terms of hydrogen overvoltage, carbon electrodes (CEs) outperform metals [6]. Carbon paste [7, 8], carbon fiber [9], glassy carbon [10], screen-printed carbon [11], carbon nanotubes (CNTs) [12, 13], and other carbon-based materials have been created and/or modified to meet particular requirements for a wide range of electrochemical applications. CNTs' nano-scale structure, excellent electrical and huge surface area, high mechanics strength, and capabilities have made them helpful in a variety of enticing applications, including nanoscale semiconductor devices, sensors, highly advanced materials, power-converting devices, and so on [14 - 17]. Several functionalization strategies have been developed to enable the application of CNTs in the fabrication of sensor electrodes [18 -21].
Conductive polymers are extensively used in electrode materials due to their superior conductivity, biological compatibility, great chemical stability, and ease of production and processing [22]. Polypyrrole (PPy) is the most extensively researched conductive polymer to date [23]. PPy has strong water stability and reasonable conductivity. Moreover, it is readily produced, and its surface features, like porosity, may easily be modified for various purposes [24]. Electrochemical impedance spectroscopy (EIS) indicated that the CNTs-PPy significantly lowered the electrode's charge transfer resistance [25].

Gold nanoparticles (AuNPs) have attracted interest in recent decades for their remarkable catalytic characteristics in various processes, including low-temperature CO oxidation. As a result, investigating the electrocatalytic activity of gold nanoparticles for O_2 reduction is critical. A two-electron reduction of oxygen occurs on Au electrodes at low overpotentials in acid environments, with the first electron transfer dictating the rate. The O_2 reduction reaction was found to be a structure-sensitive reaction on gold electrodes [26, 27].

This study aimed to assess the adsorption and electrooxidation of indium tin oxide (ITO) working electrodes (WE) modified with Multiwall Carbon Nanotubes (MWCNTs) functionalized with Polypyrrole polymer (PPy) (at different concentrations (0.02, 0.04, and 0.1 mL)) and gold nanoparticles (AuNPs) in order to modify the working electrode (ITO/f-MWCNTs-PPyAuNPs) to develop a genosensor.

2. Experimental Work

2-1 Materials

This work employed short functionalized MWCNTs (f-MWCNTs) with 5.3-5.85% OH supplied by Nanostructured and Amorphous Materials, Texas, USA. f-MWCNTs have an outer diameter of 8 nm, a length of 0.5-2 nm, and a purity of >95.1%. Gold nanoparticles (AuNPs) with purity of >99.97%, APS: 28nm, bulk density ~ 0.85 g/m^3 were supplied by US Research Nanomaterials, Inc. Dimethyl sulfoxide (DMSO) solution with a molecular weight of 78.14 (g/mol), 99.6% purity and formula $(CH_3)_2SO$ was supplied by ALPHA CHEMIKA, India. While N, N Dimethylformamide (DMF) solution with a molecular weight of 73.08(g/mol), density of 0.944 gm/ml (at 25 °C) and formula C_3H_7NO used to prepare f-MWCNTs-PPy-AuNPs suspension, was supplied by Biosolve, USA Company. For the electrolyte solution, potassium ferrocyanide ($Fe(CN)_6]^{-3/-4}$) of 99 % purity from Sigma-Aldrich and potassium chloride (KCl) of 99 % purity from Sigma-Aldrich were used. The chemicals were utilized as received without further purification.

2-2 Preparation of (ITO/MWCNTs-PPy-AuNPs) modified electrode

For the preparation of f-MWCNTs-AuNPs suspension, 2 mg of f-MWCNTs powder was mixed with 2.0 mL of DMF solution and sonicated for 15 min. with a sonicated probe, then 2 µg of AuNPs were added to the suspension and sonicated again for 15 min. for a homogenous distribution. Polypyrrole conductive polymer was prepared through easy and low-cost in-situ chemical oxidative polymerization, as described by Taradh and Saleh [15] and Ahmed and Hassan [28]. By micro syringing, a quantity of PPy solution was injected directly into the (f-MWCNTs-AuNPs) prepared suspension. The breaking up of f-MWCNTs aggregation and generating a small network was accomplished by sonicating the mixture for 20 min. using an ultrasonic probe, as shown in Figure 1.

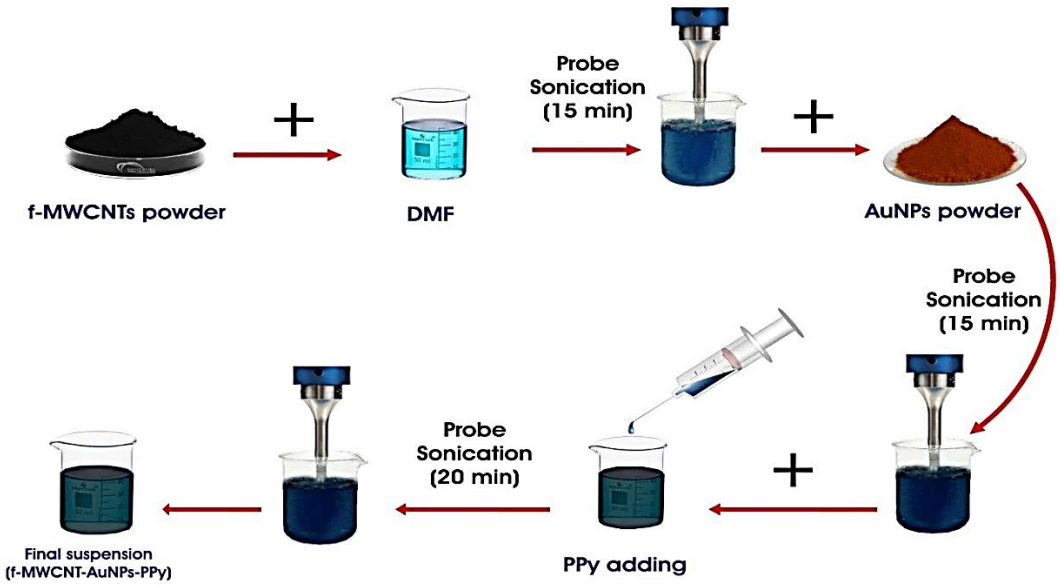

Figure 1: Schematic diagram of the (f-MWCNTs-PPy -AuNPs) suspension preparation steps.

Following that, a micropipette was used to drop 7 µL of the suspension onto the ITO surface. The (ITO/MWCNTs-PPy-AuNPs) modified electrode was successfully constructed after drying at room temperature. The schematic representation of the constructed modified electrode is shown in Figure 2.

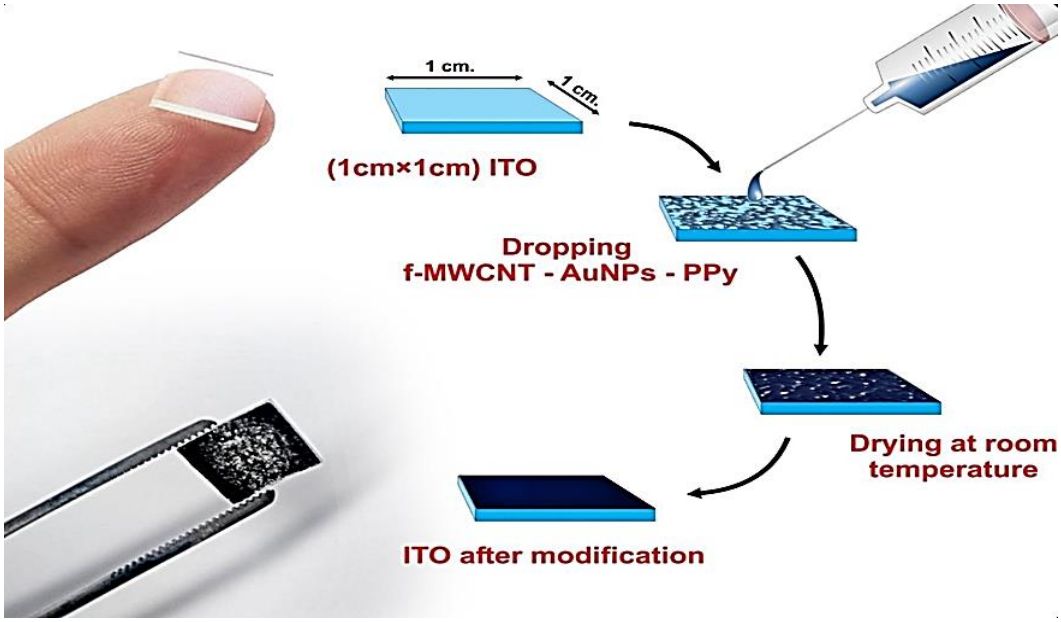

Figure 2: Schematic diagram of the proposed ITO electrode modification steps.

3. Results and discussion

3.1. Physical characterization

The produced suspension's FTIR spectra were measured in the range (500-4000) cm^{-1} using a Thermo Nicolet Avatar 360 FT-IR Spectrometer. FTIR spectra of several electrodes are presented in Figure 3.

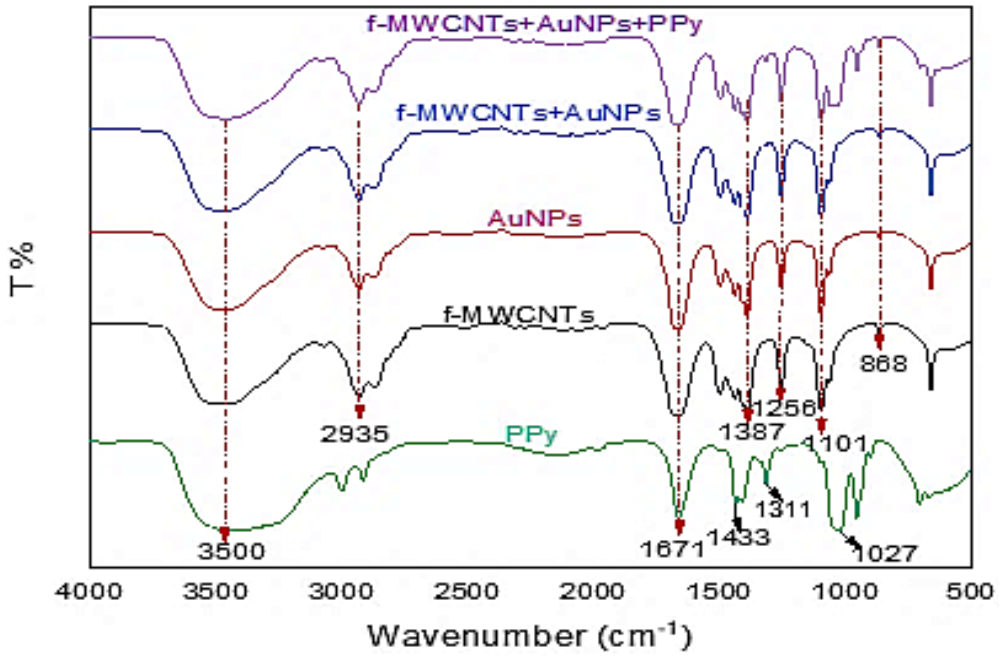

Figure 3: FTIR spectra of PPy, f-MWCNTs, AuNPs, f-MWCNTs-AuNPs, and f-MWCNTs-PPy -AuNPs.

Peaks of the PPy spectrum located at 1027cm^{-1}, 1311 cm^{-1}, 1671 cm^{-1} and 1433 cm^{-1} might be ascribed to C-H (alkene bending), C≡C and C=C deformation vibrations, C-N stretching, and antisymmetric and symmetric ring-stretching modes, respectively. The small peaks at 1671cm^{-1} in all spectra are attributed to the C=O stretching bond and are most likely attributable to PPy and f-MWCNT impurities. The wide peak at 3500 cm^{-1} in all spectra belongs to the stretching vibration of the O-H carbonyl and hydroxyl functional groups. In the spectrums of (f-MWCNTs/AuNPs/f-MWCNTs-AuNPs/MWCNTs-AuNPs-PPy) the peak at 1256 cm^{-1} is related to C-C stretching vibration. Furthermore, the weak peaks around 2935 cm^{-1} belong to C-N vibration. These results are in good agreement with the results of Alagappan et al. [29].

The capacitance of the ITO electrode material is proportional to its surface area. When comparing f-MWCNTs-AuNPs and f-MWCNTs-PPy-AuNPs, the synergistic effect of f-MWCNTs-AuNPs' high conductivity and surface area, in addition to PPy's mesoporous structure can boost the capacitance of PPy coated f-MWCNTs-AuNPs nanocomposites. Figure 4 shows FE-SEM images collected at high magnification to assess the coating state of the f-MWCNTs-AuNPs by PPy. Figure 4a shows a homogenous f-MWCNTs layer with well-dispersed AuNPs on the modified ITO electrode's surface. Figure 4b shows a thick covering of PPy on the f-MWCNTs-AuNPs nanocomposite. This might be because of the presence of more pyrrole during the in-situ polymerization procedure, which supports the generation of PPy on the surface of the f-MWCNTs-AuNPs, resulting in the thick coating [15, 30].

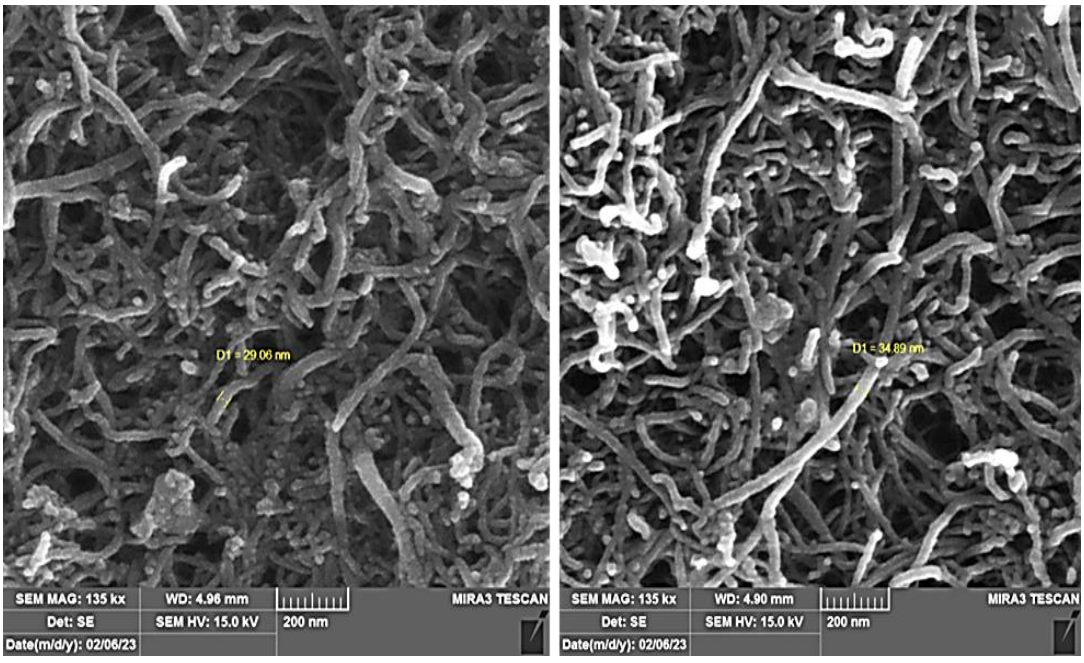

(a) **(b)**

Figure 4: FE-SEM images of (a): f-MWCNTs-AuNPs and (b) f-MWCNTs-AuNPs-PPy films deposited on ITO conductive glass.

3.2 Electrochemical characterization

In this study, voltammetric measurements were done with an IRASOl PGS-10 potentiostat/galvanostat operated by LMS-27 software. In electrochemical testing, a 200 mL electrochemical cell with a modified ITO WE, an Ag/AgCl reference electrode (RE) and a platinum wire counter electrode (CE) were used. Electrochemical Impedance Spectroscopy (EIS) investigations were carried out with a PGS-18 potentiostat.

Figure 5 shows the Cyclic Voltammetry (CV) of the modified electrodes and the ITO electrode in 10 mM $[Fe(CN)_6]^{-3/-4}$ in 0.1 M KCl solution, at (-0.5 − 1.2) V potential range with a scan rate of 100 mV/s. The ITO electrode exhibited very low capacitive current and no Faradic current in the applied potential range. The capacitive current increased when the surface was coated with f-MWCNTs because the electroactive area increased due to the presence of carbon nanotubes. The cathodic and anodic peaks associated with the redox reactions of the carboxylic acid groups were also clearly visible.
When the electrode was modified with f-MWCNTs-PPy-AuNPs, the current associated with carboxylic acid group redox processes rose compared to ITO and f-MWCNTs. This behavior might be due to the f-MWCNTs-PPy layer's high conductivity, huge specific surface area, and the catalytic influence of AuNPs, which accelerates electron transmission. The various electrochemical responses recorded using cyclic voltammetry give insight into the diverse spatial conformations selected by AuNPs on f-MWCNTs depending on the functionalization technique.

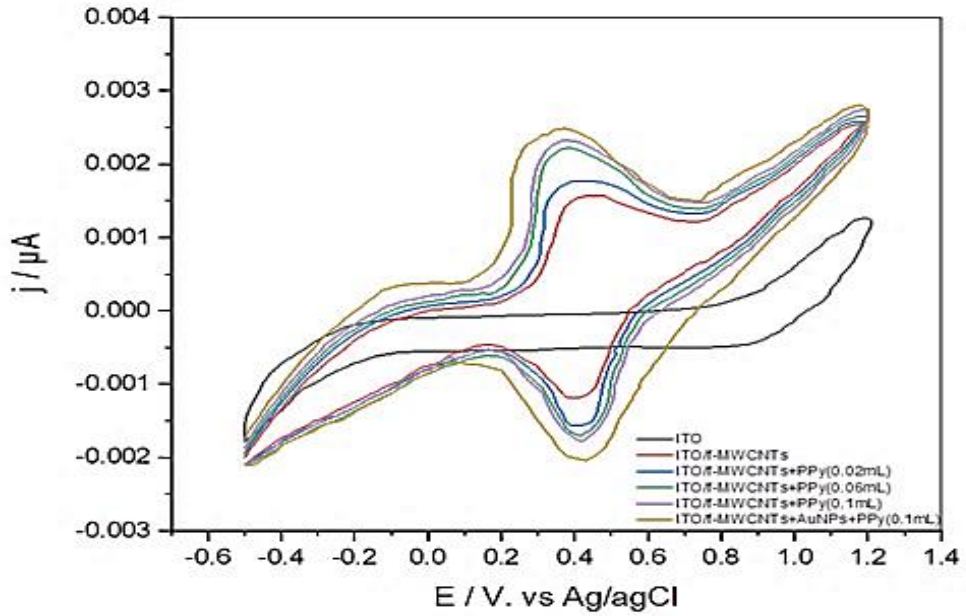

Figure 5: Cyclic voltammograms for ITO, f-MWCNTs, f-MWCNTs-PPy(0.02mL), f-MWCNTs-PPy(0.06mL), f-MWCNTs-PPy(0.1mL) and f-MWCNTs-AuNPs-PPy(0.1mL).

This conformational shift of the AuNPs on the f-MWCNTs impacts the dispersion homogeneity and, as a result, the surface characteristics of the electrode. These findings are consistent with previous research and suggest that the MWCNTs-PPy-AuNPs generated might be used in genosensor applications [31, 32].

In Electrochemical Impedance Spectroscopy (EIS), data collected from measurements are fitted to an equivalent electrical circuit model specified circuit to identify its characteristics.
Figure 6 depicts the Constant Phase Element with two layers (CPE), a circuit model in which R_s indicates the resistance of the solution, Z_D indicates the diffusion impedance and R_{ct} indicates the resistance of the charge transfer. Z_{CPE} is the impedance of a capacitor expressed as [33, 34]:

$$Z_{CPE} = \frac{1}{q}(t\omega)^{-n}$$

Where: q represents the capacitance when n is approximated to 1, $t=\sqrt{-1}$, $\omega= 2\pi f$ (rad/s) represents the angular frequency, and f is the frequency (Hz). The parameter n determines the

distribution of the phase-phase interaction where (0 < n < 1). The impedance matches the Warburg impedance at n = 0.5, and the CPE resembles a capacitor when n=1.
High-frequency semicircle-like complex plane plots were identified in all modified ITO electrodes, but the line of lower frequency became significantly larger as a result of surface preparation and deposition of f-MWCNTs. At low frequencies, the Nyquist plots revealed a slanted line similar to Warburg impedance, but the diffusive impedance, which is mainly associated with the line of transmission model, was utilized to represent the diffusion process's impedance response. Many systems in which charge transfer is governed by a diffusion process have been investigated using this model [35-37].

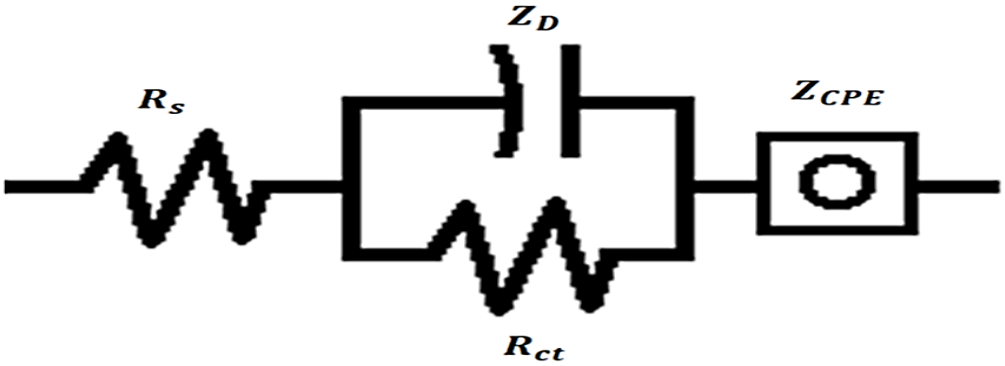

Figure 6: Equivalent electrical circuit used in EIS fitting data for electrodes.

Nyquist plots, shown in Figure 7, were obtained at 0.2 V at a frequency range (0.1 - 100) KHz. An equivalent electrical circuit was built employing ZSimpWin software using the impedance spectra. An indicator of the electrode modification process is the difference in charge transfer resistance R_{ct} values which were determined for each stage of electrode change(Table 1). The presence of f-MWCNTs increases electron transmission due to disrupted sp^2 bonding networks, explaining the reduction in R_{ct} value to 0.059KΩ after drop-casting of f-MWCNTs on the ITO electrode. Adding PPy at different concentrations (0.02, 0.04, and 0.1 mL) to f-MWCNTs reduced the R_{ct} value to 0.055KΩ, 0.043KΩ and 0.038 KΩ, respectively. Whereas, the addition of AuNPs to f-MWCNTs-PPy (at 0.1mL PPy) lowered the R_{ct}value to 0.029KΩ due to the total covering of the gold nanoparticles.

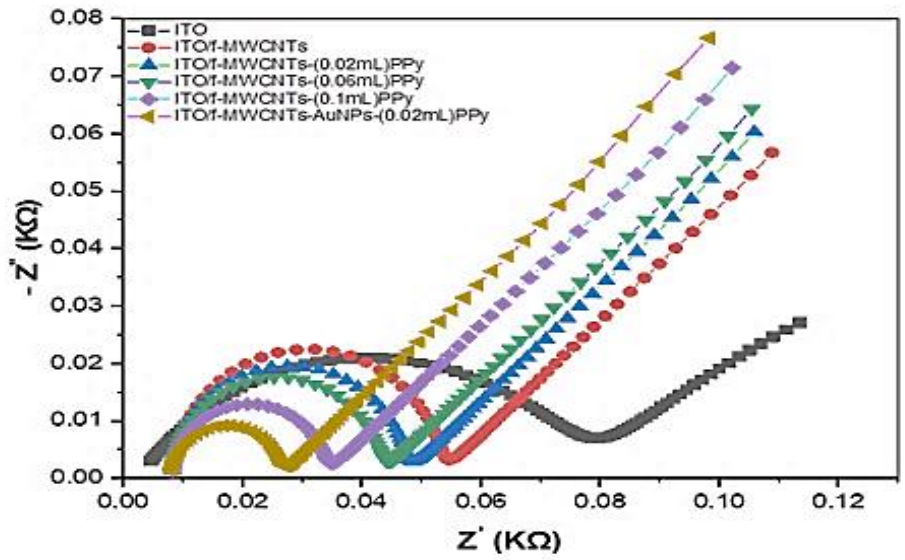

Figure 7: Nyquist diagrams of the ITO electrode before and after modificationin (10 mM) $[Fe(CN)_6]^{-3/-4}$ in (0.1 M) KCl.

As a consequence, the equivalent circuit model shown in Figure 6 utilized to clarify the form of the EIS spectra indicated that the disorderly line detected at lower frequencies was driven by a dispersed transfer mechanism. Furthermore, the total impact of charge transfer in bulk, electrode/liquid interfaces, and the solid phase all have the electrochemical reactions of ITO electrodes in a wide frequency range. ΔE in Table 1 represents the difference between the potential of redoxing electrons. It is another indication of the modification process. The best result was when ΔE is approximately equal to zero, which be because the oxidation and reduction energies of the electrons are convergent.

Table 1: The characteristic parameters of CV and EIS of the proposed modified electrode during different steps of its preparation

NO.	Modified electrode	I_{Red} (µA)	I_{Ox} (µA)	ΔE (V)	R_{ct} (KΩ)
1	Bare ITO	--------	--------	-------	0.072
2	f-MWCNTs	-0.00118	0.00158	0.0172	0.059
3	f-MWCNTs-PPy(0.02mL)	-0.00153	0.00179	0.0215	0.055
4	f-MWCNTs-PPy(0.06mL)	-0.00168	0.00221	0.0560	0.043
5	f-MWCNTs-PPy(0.1mL)	-0.00178	0.00233	0.0517	0.038
6	f-MWCNTs-AuNPs-PPy(0.1mL)	-0.00202	0.00243	0.0766	0.029

According to Table 1, the modified ITO electrode with the best electrochemical sensing was f-MWCNTs-AuNPs-PPy(0.1mL), because it has a greater oxidation current, lower reduction current, as well as lower charge transfer resistance.

Conclusions

A nanostructured material based on functionalized multiwall carbon nanotubes, gold nanoparticles, and Polypyrrole was successfully built for the production of electrochemical genosensors that make use of the synergistic benefits of nanomaterials and a conductive polymer.

The electrochemical activity of the modified ITO electrode surface was studied using EIS and CV in the presence of various redox mediators. A significant improvement in thin film performance was observed using different procedures for modifying the electrode surface, owing to previously reported conductive features and catalytic characteristics of nanomaterials and conductive polymer. Based on these findings, the projected benefits and high potential of using nanomaterials and polymers to modify the electrode surface to manufacture electrochemical genosensors were proven.

The technique provided in this study offers substantial future possibilities for biosensors in the clinical-medical, environmental, and food application sectors.

Acknowledgments

The authors would like to thank the staff of the laboratory of Laser and Electro-Optics, Department of Physics, College of Science, University of Baghdad, for their contribution to the success of this work.

References

[1] R. H. Althomali, K. A. Alamry, M. A. Hussein, and R. M. Guedes, "Hybrid pani@dialdehyde carboxymethyl cellulose/ZnO nanocomposite modified glassy carbon electrode as a highly sensitive electrochemical sensor," *Diamond and Related Materials*, vol. 122, p. 108803, 2022. doi:10.1016/j.diamond.2021.108803.

[2] A. Seifi, A. Afkhami, and T. Madrakian, "Highly sensitive and simultaneous electrochemical determination of lead and cadmium ions by poly(thionine)/MWCNTs-modified glassy carbon

electrode in the presence of bismuth ions," *Journal of Applied Electrochemistry*, vol. 52, no. 10, pp. 1513–1523, 2022. doi:10.1007/s10800-022-01728-4.

[3] E. Pajootan and M. Arami, "Structural and electrochemical characterization of carbon electrode modified by multi-walled carbon nanotubes and surfactant," *Electrochimica Acta*, vol. 112, pp. 505–514, 2013. doi:10.1016/j.electacta.2013.09.012.

[4] A. M. Abdel-Aziz, H. H. Hassan, and I. H. Badr, "Activated glassy carbon electrode as an electrochemical sensing platform for the determination of 4-nitrophenol and dopamine in real samples," *ACS Omega*, vol. 7, no. 38, pp. 34127–34135, 2022. doi:10.1021/acsomega.2c03427.

[5] M. F. Umar, A. Nasar, and Inamuddin, "Polythiophene/multiwalled carbon nanotubes/nitrate reductase deposited glassy carbon electrode (GCE/PTH/MWCNT/NR): A Novel Biosensor for the detection of nitrate in aqueous solution," *Water Supply*, vol. 22, no. 11, pp. 8023–8035, 2022. doi:10.2166/ws.2022.334 .

[6] A. Kassa, M. Amare, A. Benor, G. T. Tigineh, Y. Beyene, M. Tefera, and A. Abebe, "Potentiodynamic Poly(resorcinol)-modified glassy carbon electrode as a voltammetric sensor for determining cephalexin and Cefadroxil simultaneously in pharmaceutical formulation and biological fluid samples," *ACS Omega*, vol. 7, no. 38, pp. 34599–34607, 2022. doi:10.1021/acsomega.2c04514.

[7] Q. Azizpour Moallem and H. Beitollahi, "Electrochemical sensor for simultaneous detection of dopamine and uric acid based on a carbon paste electrode modified with nanostructured Cu-based metal-organic frameworks," *Microchemical Journal*, vol. 177, p. 107261, 2022. doi:10.1016/j.microc.2022.107261.

[8] J. A. Cruz-Navarro, L. H. Mendoza-Huizar, V. Salazar-Pereda, C. Romo-Gómez, J. Á. Cobos-Murcia, and G. A. Álvarez-Romero, "A Cu(ii)-btc metal-organic framework modified carbon paste electrode and its application as electrochemical sensor for methanol determination," *Journal of The Electrochemical Society*, vol. 169, no. 3, p. 037509, 2022.

[9] L. Ouyang, J. Liu, Y. Xiao, Y. Zhang, G. Xie, H. Zhang, and Z. Yu, "One-step preparation of a superhydrophobic surface by electric discharge machining with a carbon fiber brush electrode," *Langmuir*, vol. 38, no. 32, pp. 9853–9862, 2022.

[10] D. C. Poudyal, V. N. Dhamu, M. Samson, S. Muthukumar, and S. Prasad, "Portable pesticide electrochem-sensor: A label-free detection of glyphosate in human urine," *Langmuir*, vol. 38, no. 5, pp. 1781–1790, 2022.

[11] J. Zhou, K. Pan, G. Qu, W. Ji, P. Ning, H. Tang, and R. Xie, "RGO/MWCNTs-COOH 3D hybrid network as a high-performance electrochemical sensing platform of screen-printed carbon electrodes with an ultra-wide detection range of CD(II) and pb(ii)," *Chemical Engineering Journal*, vol. 449, p. 137853, 2022.

[12] M. Nodehi, M. Baghayeri, and A. Kaffash, "Application of BiNPs /MWCNTs-PDA/GC sensor to measurement of TL (1) and Pb (ii) using stripping voltammetry," *Chemosphere*, vol. 301, p. 134701, 2022.

[13] A. Dehdashti and A. Babaei, "Highly sensitive electrochemical sensor based on PT doped NiO nanoparticles/MWCNTs nanocomposite modified electrode for simultaneous sensing of Piroxicam and Amlodipine," *Electroanalysis*, vol. 32, no. 5, pp. 1017–1024, 2020.

[14] A. G. Enad, E. T. Abdullah, and M. G. Hamed, "Study the electrical properties of carbon nanotubes/polyaniline nanocomposites," *Journal of Physics: Conference Series*, vol. 1178, p. 012032, 2019.

[15] A. Y. Taradh and W. R. Saleh, "Fabrication and characterization of functionalized multi-wall carbon nanotubes flexible network modified by a layer of polypyrrole conductive polymer and metallic nanoparticles," *Nano Hybrids and Composites*, vol. 36, pp. 21–33, 2022.

[16] W. R. Saleh, "A carbon nanotubes photoconductive detector for middle and far infrared regions based on porous silicon and a polyamide nylon polymer," *The European Physical Journal Applied Physics*, vol. 70, no. 3, p. 30401, 2015.

[17] B. Y. Kadem, R. K. Husein, and Z. Y. Abbas, "Copper phthalocyanine MWCNTs composites: Characterization and evaluation for sensor and solar cells interlayer," *Iraqi Journal of Science*, pp. 3373–3381, 2022. doi:10.24996/ijs.2022.63.8.13.

[18] M. V. Kharlamova, M. Paukov, and M. G. Burdanova, "Nanotube functionalization: Investigation, methods and demonstrated applications," *Materials*, vol. 15, no. 15, p. 5386, 2022.

[19] H. Hosseini and M. Ghaffarzadeh, "Surface functionalization of carbon nanotubes via plasma discharge: A Review," *Inorganic Chemistry Communications*, vol. 138, p. 109276, 2022.

[20] D. C. Ferrier and K. C. Honeychurch, "Carbon Nanotube (CNT)-based biosensors," *Biosensors*, vol. 11, no. 12, p. 486, 2021.

[21] M. H. Raheema, "Coating of carbon nanotubes using chemical method to enhance the corrosion protection of copper and aluminum metals in seawater medium," *Iraqi Journal of Science*, vol. 64, no. 5, pp. 2117–2128, 2023. doi:10.24996/ijs.2023.64.5.1.

[22] S. Kalathil and D. Pant, "Nanotechnology to rescue bacterial bidirectional extracellular electron transfer in bioelectrochemical systems," *RSC Advances*, vol. 6, no. 36, pp. 30582–30597, 2016.

[23] N. Sultana, "*Stimulus-receptive conductive polymers for tissue engineering*," in Tissue Engineering Strategies for Organ Regeneration, Naznin Sultana, Sanchita Bandyopadhyay-Ghosh, and Chin Fhong Soon(Eds.),1st ed., CRC Press, 2020, p. 144156.

[24] Geetanjali, S. K. Dhillon, and P. P. Kundu, "Development of polypyrrole nanotube coated with chitosan and nickel oxide as a biocompatible anode to enhance the power generation in microbial fuel cell," *Journal of Power Sources*, vol. 539, p. 231595, 2022.

[25] C. Ye, X. Chen, D. Zhang, J. Xu, H. Xi, T. Wu, D. Deng, C. Xiong, J. Zhang, and G. Huang, "Study on the properties and reaction mechanism of polypyrrole@norfloxacin molecularly imprinted electrochemical sensor based on three-dimensional CoFe-MoFs/AuNPs," *Electrochimica Acta*, vol. 379, p. 138174, 2021.

[26] A. Saki, Z. Pourghobadi, and Z. Derikvand, "Gold nanoparticles decorated with multi-walled carbon nanotubes/graphene oxide for voltammetric determination of dopamine in the presence of acetaminophen," *Journal of The Electrochemical Society*, vol. 169, no. 11, p. 116507, 2022.

[27] K. Saeedfar, L. Y. Heng, and C. P. Chiang, "A DNA biosensor based on gold nanoparticle decorated on carboxylated multi-walled carbon nanotubes for gender determination of Arowana Fish," *Bioelectrochemistry*, vol. 118, pp. 106–113, 2017.

[28] F. M. Ahmed and S. M. Hassan, "Optical and A.C. Electrical Properties for polypyrrole and polypyrrole/graphene (PPy/GN) nanocomposites," *Iraqi Journal of Physics*, vol. 19, no. 51, pp. 72–78, 2021.

[29] M. Alagappan, S. Immanuel, R. Sivasubramanian, and A. Kandaswamy, "Development of cholesterol biosensor using Au nanoparticles decorated F-MWCNT covered with Polypyrrole Network," *Arabian Journal of Chemistry*, vol. 13, no. 1, pp. 2001–2010, 2020.

[30] A. Madhan Kumar, P. Sudhagar, A. Fujishima, and Z. M. Gasem, "Hierarchical polymer nanocomposite coating material for 316l SS implants: Surface and electrochemical aspects of PPy/F-CNTs coatings," *Polymer*, vol. 55, no. 21, pp. 5417–5424, 2014. doi:10.1016/j.polymer.2014.08.073.

[31] Y. Ye, W. Yan, Y. Liu, S. He, X. Cao, X. Xu, H. Zheng, and S. Gunasekaran, "Electrochemical detection of salmonella using an INVA genosensor on polypyrrole-reduced graphene oxide modified glassy carbon electrode and aunps-horseradish peroxidase-streptavidin as nanotag," *Analytica Chimica Acta*, vol. 1074, pp. 80–88, 2019.

[32] A. F. Quintero-Jaime, D. Cazorla-Amorós, and E. Morallón, "Effect of surface oxygen groups in the electrochemical modification of multi-walled carbon nanotubes by 4-amino phenyl phosphonic acid," *Carbon*, vol. 165, pp. 328–339, 2020.

[33] H. Zhou, T. Wang, and Y. Y. Duan, "A simple method for amino-functionalization of carbon nanotubes and electrodeposition to modify neural microelectrodes," *Journal of Electroanalytical Chemistry*, vol. 688, pp. 69–75, 2013.

[34] Y. Y. Duan, G. M. Clark, and R. S. C. Cowan, "A study of intra-cochlear electrodes and tissue interface by electrochemical impedance methods in vivo," *Biomaterials*, vol. 25, no. 17, pp. 3813–3828, 2004.

[35] J. Bisquert and A. Compte, "Theory of the electrochemical impedance of Anomalous Diffusion," *Journal of Electroanalytical Chemistry*, vol. 499, no. 1, pp. 112–120, 2001.

[36] J. Bisquert, G. Garcia-Belmonte, F. Fabregat-Santiago, and P. R. Bueno, "Theoretical models for AC impedance of finite diffusion layers exhibiting low frequency dispersion," *Journal of Electroanalytical Chemistry*, vol. 475, no. 2, pp. 152–163, 1999.

[37] G. Garcia-Belmonte, Z. Pomerantz, J. Bisquert, J.-P. Lellouche, and A. Zaban, "Analysis of Ion Diffusion and charging in electronically conducting polydicarbazole films by impedance methods," *Electrochimica Acta*, vol. 49, no. 20, pp. 3413–3417, 2004.